Fatigue Crack Initiation in Carbon and Low-Alloy Steels in Light Water Reactor Environments: Mechanism and Prediction*

Omesh K. Chopra and William J. Shack

Energy Technology Division
Argonne National Laboratory
9700 South Cass Avenue
Argonne, Illinois 60439 USA

December 1997

To be presented at the *Symposium on Fatigue & Fracture in Pressure Vessels and Piping*, 1998 ASME/JSME Joint Pressure Vessel and Piping Conference, July 26–30, 1998, Sheraton San Diego Hotel and Marina, San Diego, CA.

---

*Work supported by the Office of Nuclear Regulatory Research of the U.S. Nuclear Regulatory Commission, under FIN Number W6610; Program Manager: Dr. M. McNeil.

DISCLAIMER

Fatigue Crack Initiation in Carbon and Low-Alloy Steels in Light Water Reactor Environments: Mechanism and Prediction

Omesh K. Chopra and William J. Shack

Energy Technology Division
Argonne National Laboratory
Argonne, Illinois 60439

ABSTRACT

Section III of the ASME Boiler and Pressure Vessel Code specifies fatigue design curves for structural materials. The effects of reactor coolant environments are not explicitly addressed by the Code design curves. Recent test data illustrate potentially significant effects of light water reactor (LWR) coolant environments on the fatigue resistance of carbon and low-alloy steels. Under certain loading and environmental conditions, fatigue lives of test specimens may be shorter than those in air by a factor of ≈70. The crack initiation and crack growth characteristics of carbon and low-alloy steels in LWR environments are presented. Decreases in fatigue life of these steels in high-dissolved-oxygen water are caused primarily by the effect of environment on growth of short cracks < 100 μm in depth. The material and loading parameters that influence fatigue life in LWR environments are defined. Fatigue life is decreased significantly when five conditions are satisfied simultaneously, viz., applied strain range, service temperature, dissolved oxygen in water, and S content in steel are above a threshold level, and loading strain rate is below a threshold value. Statistical models have been developed for estimating the fatigue life of these steels in LWR environments. The significance of the effect of environment on the current Code design curve is evaluated.

INTRODUCTION

Cyclic loadings on a structural component occur because of changes in the mechanical and thermal loadings as the system goes from one load set (e.g., pressure, temperature, moment, and force loading) to any other load set. For each pair of load set, an individual fatigue usage factor is determined by the ratio of the number of cycles anticipated during the lifetime of the component to the allowable cycles. Figures I-9.1 through I-9.6 of Appendix I to Section III of the ASME Boiler and Pressure Vessel Code specify fatigue design curves that define the allowable number of cycles as a function of applied stress amplitude. The cumulative usage factor (CUF) is the sum of the individual usage factors, and the ASME Code Section III requires that the CUF at each location must not exceed 1.

The Code design fatigue curves were based on strain-controlled tests of small polished specimens at room temperature (RT) in air. The design fatigue curves were obtained by decreasing the best-fit curves to the experimental data by a factor of 2 on strain or 20 on cycles, whichever was more conservative, at each point on the best-fit curve. As described in the Section III criteria document, these factors were intended to account for the differences and uncertainties in relating the fatigue lives of laboratory test specimens to those of actual reactor components. The factors of 2 and 20 are not safety margins but rather conversion factors that must be applied to the experimental data to obtain reasonable estimates of the lives of actual reactor components (in a benign environment some fraction, e.g., ≈25%, of the factors is available as a safety margin).

Subsection NB-3121 of Section III of the Code states that the data on which the fatigue design curves are based did not include tests in the presence of corrosive environments that might accelerate fatigue failure. Article B-2131 in Appendix B to Section III states that the owner's design specifications should provide information on any reduction to fatigue design curves necessitated by environmental conditions. Recent fatigue strain-vs.-life (S-N) data illustrate potentially significant effects of light water reactor (LWR) coolant environments on the fatigue resistance of carbon steels (CSs) and low-alloy steels (LASs).[1-5] Specimen lives in simulated LWR environments can be much shorter than those for corresponding tests in air. Under certain conditions of loading and environment, fatigue lives of carbon steels can be a factor of 70 lower in the environment than those in air. These results raise the issue of whether the fatigue design curves in Section III are appropriate for the purposes intended and whether they adequately account for environmental effects on fatigue behavior.

This paper presents the existing fatigue S-N data for carbon and low-alloy steels in LWR environments. The effects of various material and loading variables such as steel type, strain range, strain rate, temperature, sulfur content in steel, orientation, and DO level in water on the fatigue life of these steels are summarized. The influence of reactor environments on the formation and growth of fatigue cracks is discussed. Statistical models have been developed for estimating the fatigue S-N curves as a function of material, loading, and environmental variables. The different methods for incorporating the effects of LWR coolant environments on the ASME Code fatigue design curves are presented.

OVERVIEW OF FATIGUE S-N DATA

The primary sources of relevant S-N data for CSs and LASs are the tests performed by General Electric Co. (GE) in a test loop at the Dresden 1 reactor;[6,7] work sponsored by EPRI at GE;[1] the work of Terrell at Mechanical Engineering Associates (MEA);[8,9] the present work at ANL on fatigue of pressure vessel and piping steels;[5,10-13] the JNUFAD* data base for "Fatigue Strength of Nuclear Plant Component" and recent studies at IHI, Hitachi, and Mitsubishi Heavy Industries in Japan.[2,14-18] The data base is composed of ≈1200 tests, ≈600 each in air and water environments. Carbon steels include ≈10 heats of A333-Grade 6, A106-Grade B, A516-Grade 70, and A508-Class 1 steel, while the LASs include ≈15 heats of A533-Grade B, A302-Gr B, and A508-Class 2 and 3 steels.

Air Environment

In air, the fatigue life of carbon and low-alloy steels depends on steel type, temperature, orientation (rolling or transverse), and strain rate. The fatigue life of carbon steels is a factor of ≈1.5 lower than that of low-alloy steels. For both steels, life is decreased by a factor of ≈1.5 when temperature is increased from room temperature to 288°C. In the temperature range of dynamic strain aging (200-370°C), some heats of carbon and low-alloy steels are sensitive to strain rate. The effect of strain rate on fatigue life is not clear; life may be unaffected, decrease for some heats, or increase for others. In this temperature range, however, cyclic stresses increase with decreasing strain rate. Also, based on the distribution and morphology of

*Private communication from M. Higuchi, Ishikawajima-Harima Heavy Industries Co., Japan, to M. Prager of the Pressure Vessel Research Council, 1992. The old data base "FADAL" has been revised and renamed "JNUFAD."

sulfides, fatigue properties in the transverse orientation may be inferior to those in the rolling orientation.

The data indicate significant heat-to-heat variation; at 288°C, fatigue life may vary up to a factor of 5 above or below the mean value. The results also indicate that the ASME mean curve for low-alloy steels is in good agreement with the experimental data and that for carbon steels it is somewhat conservative. At strain amplitudes of <0.2%, the mean curve for CSs predicts significantly lower fatigue lives than those observed experimentally.

LWR Environments

The fatigue life of both carbon and low-alloy steels is decreased significantly when five conditions are satisfied simultaneously, viz., applied strain amplitude, service temperature, DO level in the water, and sulfur content of the steel are above a minimum threshold level, and the loading strain rate is below a threshold value. Although the microstructures and cyclic-hardening behavior of CSs and LASs are significantly different, environmental degradation of fatigue life of these steels is identical. For both steels, only moderate decrease in life (by a factor of less than 2) is observed when any one of these conditions is not satisfied. The effects of various material and loading parameters on fatigue life and the threshold values of the critical parameters are summarized below.

(a) *Strain Amplitude*: A minimum threshold strain is required for environmentally assisted decrease in fatigue life of these steels.[5,10,11] This behavior is consistent with the slip oxidation/dissolution mechanism[19] for enhancement of crack growth rates; threshold strain most likely corresponds to the rupture strain of the surface oxide film. Limited data suggest that the threshold value is ≈20% higher than the fatigue limit for the steel.[5]

(b) *Strain Rate*: When any one of the threshold conditions is not satisfied, e.g., DO <0.05 ppm or temperature <150°C, the effects of strain rate are consistent with those in air, i.e., heats that are sensitive to strain rate in air, also show a decrease in life in water. When all other threshold conditions are satisfied, fatigue life decreases logarithmically with decreasing strain rate below 1%/s; the effect of environment saturates at ≈0.001%/s.[2,5,15,17]

(c) *Loading Cycle*: Environmental effects on fatigue life occur primarily during the tensile-loading cycle, and at strain levels greater than the threshold value required to rupture the surface oxide film. Compressive-loading cycle has little or no effect on life. Results from exploratory tests,[5,16] where the slow strain rate is applied during only a fraction of the tensile loading cycle, indicate that the relative damage due to slow strain rate is independent of strain amplitude once the amplitude exceeds a threshold value to rupture the passive surface film. Consequently, loading and environmental conditions, e.g., strain rate, temperature, and DO level, during the tensile-loading cycle in excess of the oxide rupture strain, are important parameters for environmentally assisted reduction in fatigue life of these steels.

(d) *Temperature*: When other threshold conditions are satisfied, fatigue life decreases linearly with temperature above 150°C and up to 320°C.[2,14,17] Fatigue life is insensitive to temperatures below 150°C or when any other threshold condition is not satisfied. Estimates of fatigue life from a trained Artificial Neural Network (ANN) also show a similar effect of temperature on the fatigue life of CSs and LASs.[20] Furthermore, experimental data from tests, where both strain and temperature were varied during each cycle,[18] indicate a threshold temperature of 150°C, below which environmental effects on life either do not occur or are insignificant. For service histories involving variable loading and environmental conditions, service temperature may be represented by the average of 150°C and the maximum temperature.

(e) *Dissolved Oxygen in Water:* When other threshold conditions are satisfied, fatigue life decreases logarithmically with DO above 0.05 ppm; the effect saturates at ≈0.5 ppm DO.[14,17] Estimates of fatigue life from a trained ANN also show a similar dependence of life on DO level.[20]

(f) *Sulfur Content in Steel:* Although sulfur content and morphology are the most important parameters that determine susceptibility of carbon and low–alloy steels to environmentally enhanced fatigue crack growth rates,[21–25] the existing fatigue S–N data are inadequate to establish unequivocally the effect of sulfur content on the fatigue life of these steels. When any one of the threshold conditions is not satisfied, environmental effects on life are minimal and relatively insensitive to changes in sulfur content. When the threshold conditions are satisfied, i.e., high–temperature and high–DO water, the fatigue life of LASs decreases with increasing sulfur content.[8,9] Limited data suggest that the effects of environment on life saturate at sulfur contents above 0.012 wt.%.[26] However, in high–temperature and high–DO water, the fatigue life of CSs seems to be insensitive to sulfur content in the range of 0.002–0.015 wt.%.* The variation in fatigue life of carbon and low–alloy steels with different sulfur contents is plotted as a function of strain rate in Fig. 1. For LASs, environmental effects on fatigue life increase with increased sulfur content, whereas the fatigue life for CSs seems to be independent of sulfur content in the range of 0.002–0.015 wt.%. The effect of sulfur on the growth of short cracks (during crack initiation) may be different than that of long cracks and should be further investigated.

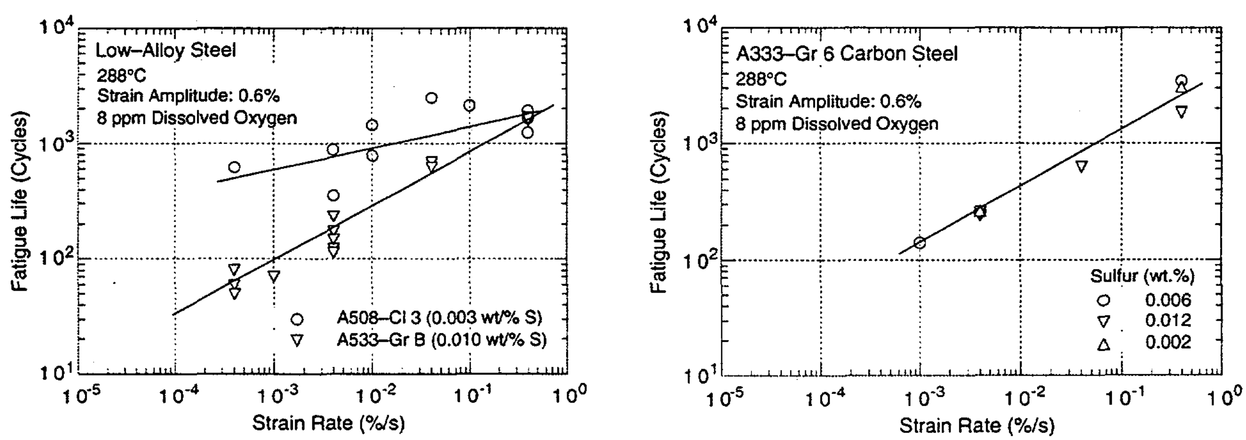

Figure 1. Effect of strain rate on fatigue life of carbon and low–alloy steels with different sulfur contents

(i) *Orientation:* The effect of orientation on fatigue life is expected because of differences in the distribution and morphology of sulfide inclusions and is well known in crack growth studies with precracked specimens.[23–25] Existing fatigue S–N data indicate that in high–

* M. Higuchi, presented at the Pressure Vessel Research Council Meeting, June 1995, Milwaukee, WI.

DO water (≤0.1 ppm DO), the fatigue life of LASs is insensitive to differences in sulfide distribution and size.[26] Sulfide morphology may influence fatigue life in low–DO PWR environments, but the difference would be insignificant because environmental effects on life are minimal in low–DO environments.

(j) *Flow Rate*: Studies on fatigue crack growth behavior of carbon and low–alloy steels indicate that flow rate is an important parameter for environmental effects on crack growth rates.[21,24,27] Corrosion fatigue growth rates are controlled by the synergistic effect of sulfur content, environmental conditions, and flow rate.[24] However, experimental data to establish either the dependence of fatigue life on flow rate or the threshold flow rate for environmental effects to occur are not available and should be developed.

MECHANISM OF FATIGUE CRACK INITIATION

The formation of surface cracks and their growth as shear and tensile cracks (Stage I and II growth) to an "engineering" size (e.g., a 3–mm–deep crack) constitute the fatigue life of a material, which is represented by the fatigue S–N curves. The curves specify, for a given stress or strain amplitude, the number of cycles needed to form an engineering crack. Fatigue life, has conventionally been represented by two stages: (a) initiation, which represents the cycles N_i for formation of microcracks on the surface; and (b) propagation, which represents cycles N_p for propagation of the surface cracks to an engineering size. Thus, fatigue life N is the sum of the two stages, $N = N_i + N_p$. The former is considered to be sensitive to the stress or strain amplitude, e.g., at low strain amplitudes, most of the life may be spent in initiating a crack, whereas at high strain amplitudes, cracks initiate easily.

The reduction in fatigue life in high–temperature water has been attributed to the presence of micropits that form in both CSs and LASs due to dissolution of MnS inclusions or by corrosion reactions and act as stress raisers and provide preferred sites for the formation of fatigue cracks.[14] If the presence of micropits was responsible for reduction in fatigue lives of carbon and low–alloy steels in LWR environments, then the following behavior should be observed: (a) specimens tested in high–DO water should show more surface cracks and (b) specimens preexposed to high–DO water and then tested in air should also show a decrease in life. Experimental data indicate the contrary. The frequency of cracks (i.e., number of cracks per unit gauge length) in CS and LAS specimens tested in air and high–DO water is identical, although fatigue life is lower by more than a factor of 8 in water.[28] Also, the fatigue lives of CS and LAS specimens preoxidized at 288°C in high–DO water (≈0.7 ppm DO) and then tested either in air or low–DO water (<0.01 ppm DO) are identical to those of unoxidized specimens.[5,10] Life would be expected to decrease if surface micropits facilitate the formation of fatigue cracks. Furthermore, if micropits were responsible for the decrease in fatigue life in LWR environments, then the fatigue limit of these steels should be lower in water than in air. Data in high–DO water indicate that the fatigue limit in water is either the same or ≈20% higher than in air. Irrespective of environment, cracks in carbon and low–alloy steels form along slip bands, carbide particles, or at ferrite/pearlite phase boundaries.[13,28]

An alternative approach considers fatigue life to be entirely composed of the growth of short fatigue cracks.[29] For polycrystalline materials, the period for the formation of surface cracks is negligible; surface cracks, 10 µm or longer, form quite early in life,[13,30,31] i.e., <10% of life even at low strain amplitudes. Fatigue damage in a material is the current size of the fatigue crack and damage accumulation is the rate of crack growth. Growth of short fatigue cracks may be divided into three regimes shown in Fig. 2a: (a) an initial period that involves growth of microstructurally small cracks (MSCs) that is very sensitive to microstructure and characterized by decelerating growth rate, region AB; (b) a final period of growth that can be predicted from fracture mechanics methodology and is characterized by accelerating crack growth rate, region CD; and (c) a transition period controlled by a combination of the two regimes, region BC.

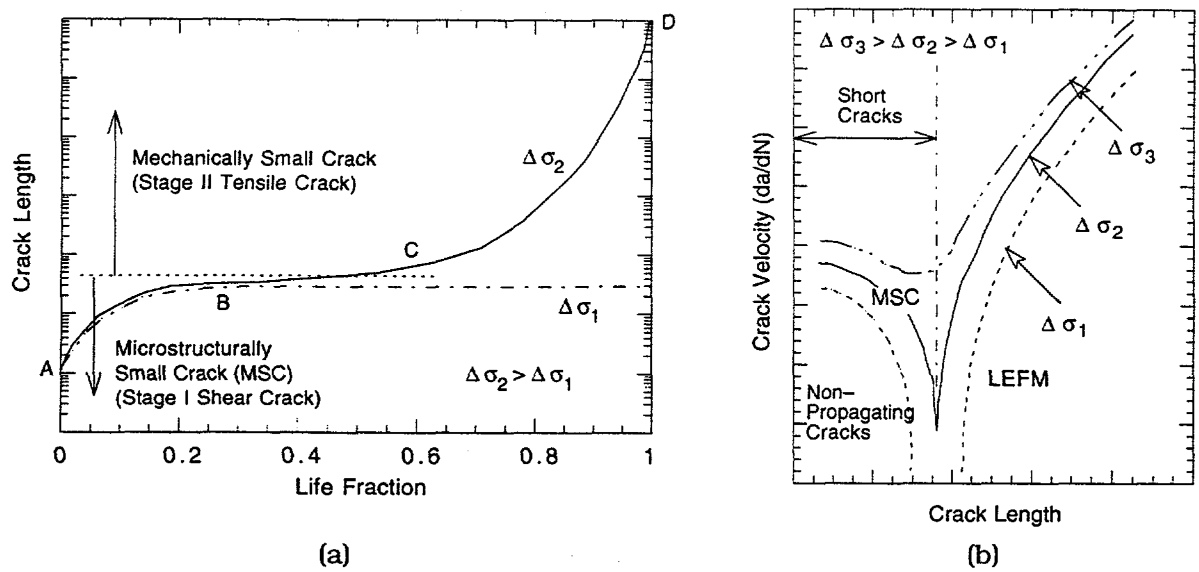

Figure 2. Schematic illustration of short crack behavior in smooth fatigue specimens (a) crack growth as a function of life fraction and (b) crack velocity as a function of crack length

The MSCs correspond to Stage I cracks and grow along slip planes as shear cracks; their growth is very sensitive to microstructure.[31–34] In ferritic–pearlitic steels, fatigue cracks initiate and propagate preferentially in the ferrite phase that forms as long allotriomorphs at prior austenite phase boundaries.[31,33,34] Fatigue cracks greater than the critical length of MSCs show little or no influence of microstructure and are termed mechanically small cracks.[32] Mechanically small cracks correspond to Stage II, or tensile, cracks characterized by striated crack growth and a fracture surface normal to the maximum principal stress. For ferritic–pearlitic steels, Stage II crack propagation occurs when stress intensity and mode of growth attain a critical level, break through the pearlite, and join other ferrite cracks.[33] At low stress levels, e.g., $\Delta\sigma_1$ in Fig. 2, the transition from MSC growth to accelerating crack growth does not occur and the cracks are nonpropagating. This circumstance represents the fatigue limit for the smooth specimen. Although cracks can form below the fatigue limit, they can grow to engineering size only at stresses greater than the fatigue limit.

Studies on the formation and growth characteristics of short cracks in smooth fatigue specimens in LWR environments indicate that the decrease in fatigue life of carbon and low–alloy steels in high–DO water is primarily caused by the effects of environment on the growth of cracks < 100 µm deep.[20] In high–temperature high–DO water, the period for region ABC in Fig. 2a is decreased or crack velocities for MSC regime in Fig. 2b are increased. Relative to air, crack growth rates in high–DO water are nearly two orders of magnitude higher during the initial stages of crack growth (for crack sizes < 100 µm), and one order of magnitude higher for crack sizes > 100 µm (Fig. 3).

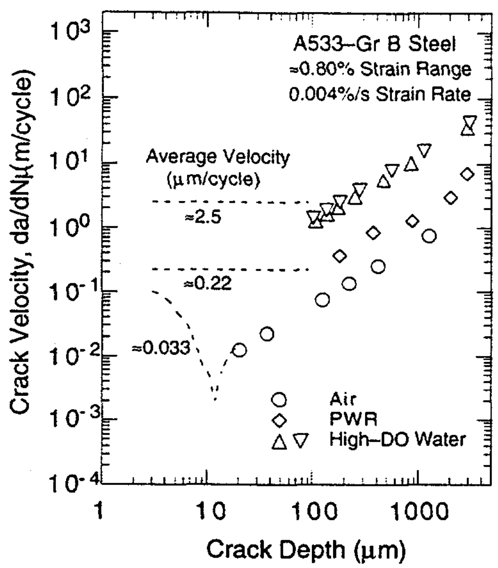

Figure 3.
Crack growth rates plotted as a function of crack depth for A533–Gr B low–alloy steel tested in air and water environments

Metallographic examination of test specimens indicate that in high–DO water, surface cracks grow entirely as tensile cracks normal to the stress;[13] for CSs, cracks propagate across both ferrite and pearlite regions. Fracture morphologies indicative of hydrogen–induced cracking, e.g., quasi–cleavage facets or fanlike features extending from sulfide inclusions or terraced morphology produced by linkage of hydrogen–induced cracks at sulfide–matrix interface ahead of the main crack,[24,35,36] are not observed in CS or LAS specimens tested in LWR environments. These results indicate that growth of MSCs occurs by slip dissolution/oxidation. In LWR environments, formation of engineering cracks may be explained as follows: (a) surface microcracks form quite early in fatigue life at PSBs, edges of slip–band extrusions, notches that develop at grain or phase boundaries, or second–phase particles; (b) during cyclic loading, the protective oxide film is ruptured at strains greater than the fracture strain of surface oxides, and the microcracks or MSCs grow by anodic dissolution of the freshly exposed surface to sizes larger than the critical length of MSCs; and (c) growth of these large cracks characterized by accelerating growth rates. The growth rates during the final stage are controlled by both environmental and mechanical factors and may be represented by the proposed ASME Section XI reference curves for CSs and LASs in water environments.[37]

STATISTICAL MODEL

The fatigue S–N curves are generally expressed in terms of the Langer equation, which may be used to represent either strain amplitude in terms of life or life in terms of strain amplitude. The parameters of the equation are commonly established through least–squares curve–fitting of the data to minimize the sum of the square of the residual errors for either strain amplitude or fatigue life. A predictive model based on least–squares fit on life is biased for low strain amplitude. The model leads to probability curves that converge to a single value of strain, and it fails to address the fact that at low strain values, most of the error in life is due to uncertainty associated with either measurement of strain or variation in fatigue limit caused by material variability. On the other hand, a least–squares fit on strain does not work well for higher strain amplitudes.

Statistical models have been developed by combining the two approaches and minimizing the sum of the squared Cartesian distances from the data point to the predicted curve.[38,39]

However, because the model includes many nonlinear transformations of variables and because different variables affect different parts of the data, the actual functional form and transformations are partly responsible for minimizing the squares of the errors. The functional forms and transformation were based on experimental observations and data trends. The models presented in Refs. 38 and 39 have been further optimized with a larger fatigue S–N data base and are described below. In air, the fatigue data for CSs are best represented by

$$\ln(N) = 6.595 - 1.975 \ln(\varepsilon_a - 0.113) - 0.00124\,T \tag{1a}$$

and for LASs by

$$\ln(N) = 6.658 - 1.808 \ln(\varepsilon_a - 0.151) - 0.00124\,T, \tag{1b}$$

where N is fatigue life of a smooth test specimen, ε_a is applied strain amplitude (%), and T is test temperature (°C). In LWR environments, the fatigue data for CSs are best represented by

$$\ln(N) = 6.010 - 1.975 \ln(\varepsilon_a - 0.113) + 0.101\,S^*\,T^*\,O^*\,\dot{\varepsilon}^* \tag{2a}$$

and for LASs by

$$\ln(N) = 5.729 - 1.808 \ln(\varepsilon_a - 0.151) + 0.101\,S^*\,T^*\,O^*\,\dot{\varepsilon}^*, \tag{2b}$$

where S^*, T^*, O^*, and $\dot{\varepsilon}^*$ = transformed sulfur content, temperature, DO, and strain rate, respectively, defined as follows:

$$\begin{array}{ll} S^* = S & (0 < S \le 0.015 \text{ wt.\%}) \\ S^* = 0.015 & (S > 0.015 \text{ wt.\%}) \end{array} \tag{3a}$$

$$\begin{array}{ll} T^* = 0 & (T < 150°C) \\ T^* = T - 150 & (T = 150\text{–}350°C) \end{array} \tag{3b}$$

$$\begin{array}{ll} O^* = 0 & (DO < 0.05 \text{ ppm}) \\ O^* = \ln(DO/0.04) & (0.05 \text{ ppm} \le DO \le 0.5 \text{ ppm}) \\ O^* = \ln(12.5) & (DO > 0.5 \text{ ppm}) \end{array} \tag{3c}$$

$$\begin{array}{ll} \dot{\varepsilon}^* = 0 & (\dot{\varepsilon} > 1\%/s) \\ \dot{\varepsilon}^* = \ln(\dot{\varepsilon}) & (0.001 \le \dot{\varepsilon} \le 1\%/s) \\ \dot{\varepsilon}^* = \ln(0.001) & (\dot{\varepsilon} < 0.001\%/s) \end{array} \tag{3d}$$

The model is recommended for predicted fatigue lives $\le 10^6$ cycles. For fatigue lives of 10^6 to 10^8 cycles, the results should be used with caution because in this range, the model is based on very limited data obtained from relatively few heats of material.

FATIGUE LIFE CORRECTION FACTOR

An alternative approach for incorporating the effects of reactor coolant environments on fatigue S–N curves has been proposed by The Environmental Fatigue Data (EFD) Committee of Thermal and Nuclear Power Engineering Society (TENPES) of Japan.* The effects of coolant environment on fatigue life are expressed in terms of a fatigue life correction factor F_{en}, which is the ratio of the life in air at room temperature to that in water at the service temperature. To

* Presented at the Pressure Vessel Research Council Meeting, April 1996, Orlando, FL.

incorporate environmental effects into the ASME Code fatigue evaluation, a fatigue usage for a specific load pair based on the current Code fatigue design curve is multiplied by the correction factor. The specific expression for F_{en}, proposed initially by Higuchi and Iida,[2] assumes that life in the environment N_{water} is related to life in air N_{air} at room temperature through a power–law dependence on the strain rate

$$F_{en} = \frac{N_{air}}{N_{water}} = (\dot{\varepsilon})^{-P} \quad (4a)$$

or $$\ln(F_{en}) = \ln(N_{air}) - \ln(N_{water}) = -P\ln(\dot{\varepsilon}). \quad (4b)$$

In air at room temperature, the fatigue life N_{air} of CSs is expressed as

$$\ln(N_{air}) = 6.653 - 2.119 \ln(\varepsilon_a - 0.108) \quad (5a)$$

and for LASs by

$$\ln(N_{air}) = 6.578 - 1.761 \ln(\varepsilon_a - 0.140), \quad (5b)$$

where ε_a is the applied strain amplitude (%). Only the tensile loading cycle is considered to be important for environmental effects on fatigue life. The exponent P is a product of an environmental factor R_p, which depends on temperature T (°C) and DO level (ppm), and a material factor P_c, which depends on the ultimate tensile strength σ_u (MPa) and sulfur content S (wt.%) of the steel. Thus

$$P = R_p P_c, \quad (6a)$$

$$P_c = 0.864 - 0.00092\,\sigma_u + 14.6\,S, \quad (6b)$$

$$R_p = \frac{R_{pT} - 0.2}{2.64}\ln(DO) + 1.75R_{pT} - 0.035, \qquad 0.2 \le R_p \le R_{pT} \quad (6c)$$

and $$R_{pT} = 0.198 \exp(0.00557T). \quad (6d)$$

The fatigue lives of carbon and low–alloy steels measured experimentally and those estimated from the statistical and EFD models are shown in Figs. 3–6. Although the EFD correlations for exponent P have been based entirely on data for CSs, Eqs. 6a–6d were also used for estimating the fatigue lives of LASs. Also, σ_u in Eq. 6b was assumed to be 520 and 650 MPa, respectively, for CSs and LASs. The significant differences between the two models are as follows: (a) EFD correlations have been developed from data for CSs alone; (b) the statistical model considers that effects of strain rate on fatigue life saturate below 0.001%/s (Fig. 5), whereas the EFD model does not consider saturation; (c) a threshold temperature of 150°C, below which environmental effects on fatigue life are modest is considered in the statistical model but not in the EFD model; and (d) EFD model includes the effect of tensile strength on the fatigue life of CSs in LWR environments. A fatigue life correction factor F_{en} can also be obtained from the statistical model, where

$$\ln(F_{en}) = \ln(N_{air}) - \ln(N_{water}). \quad (7)$$

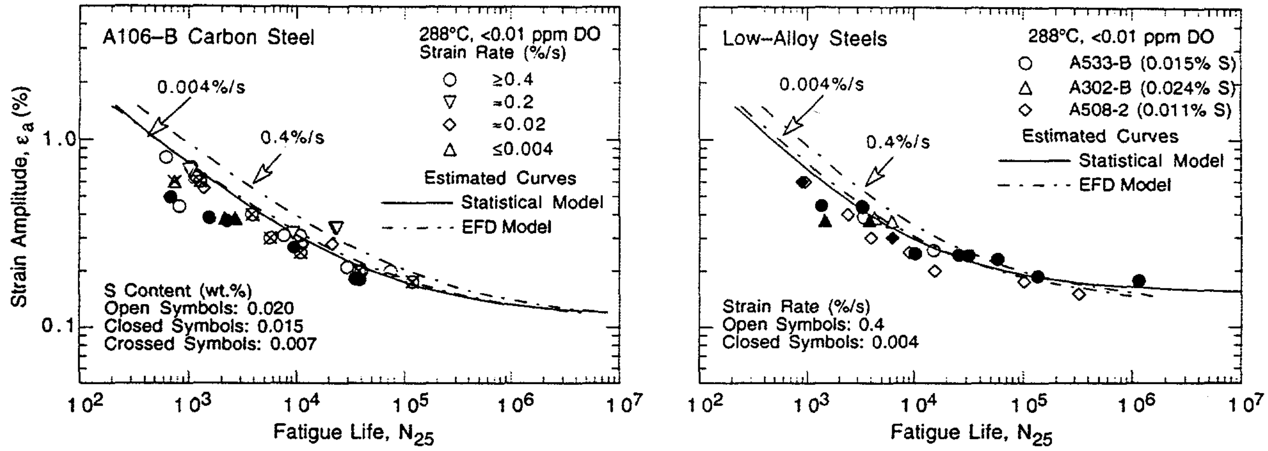

Figure 3. Experimental fatigue lives and those estimated from statistical and EFD models for carbon and low–alloy steels in simulated PWR water

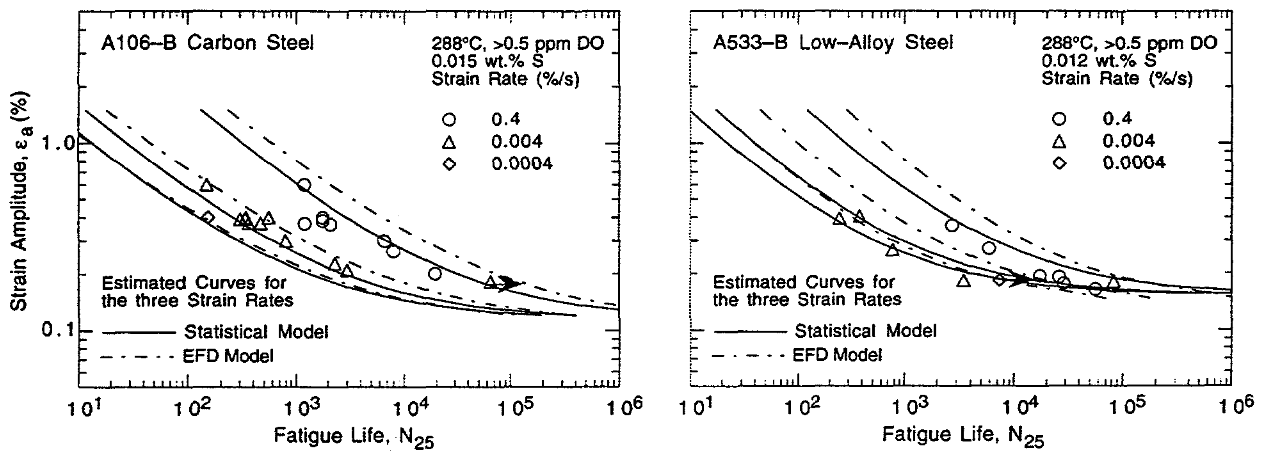

Figure 4. Experimental fatigue lives and those estimated from statistical and EFD models for carbon and low–alloy steels in high–dissolved–oxygen water

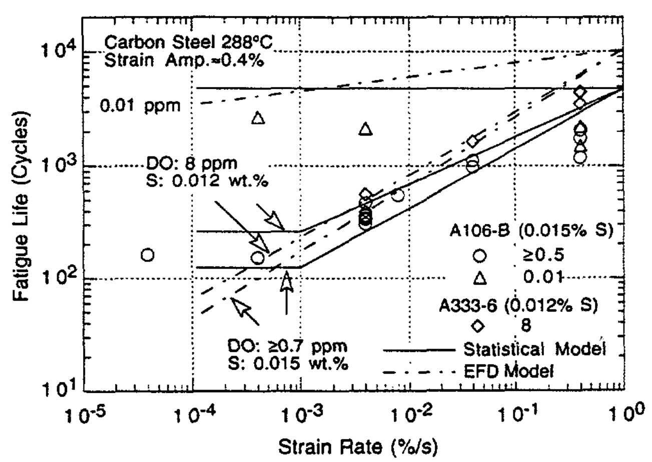

Figure 5.
Dependence on strain rate of fatigue life of carbon steels observed experimentally and that estimated from statistical and EFD models

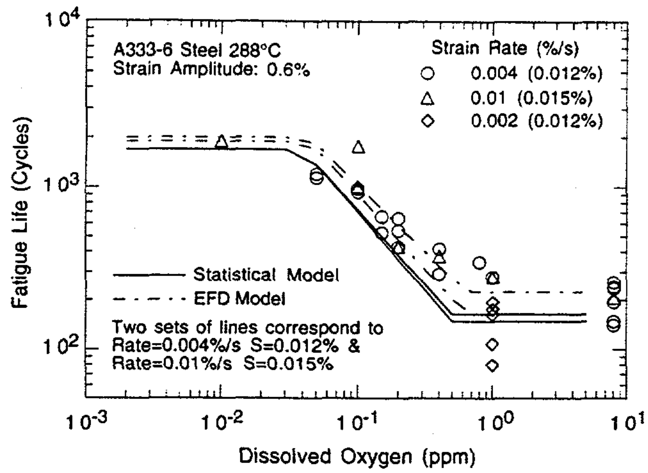

Figure 6.
Dependence on dissolved oxygen of fatigue life of carbon steels observed experimentally and that estimated from statistical and EFD models

From Eqs. 1a and 2a, the fatigue life correction factor for CSs is given by

$$\ln(F_{en}) = 0.585 - 0.00124T - 0.101S^*T^*O^*\dot{\varepsilon}^* \quad (8a)$$

and from Eqs. 1b and 2b, the fatigue life correction factor for LASs is given by

$$\ln(F_{en}) = 0.929 - 0.00124T - 0.101S^*T^*O^*\dot{\varepsilon}^*, \quad (8b)$$

where the threshold and saturation values for S^*, T^*, O^*, and $\dot{\varepsilon}^*$ are defined in Eqs. 3a–3d. A value of 25°C is used for T in Eqs. 8a and 8b if the fatigue life correction factor is defined relative to RT air. Otherwise, both T and T^* represent the service temperature. A fatigue life correction factor F_{en} based on the statistical model has been proposed for ASME Section XI fatigue evaluations.[40]

DESIGN FATIGUE CURVES

The current ASME Section III Code design fatigue curves were based on experimental data on small polished test specimens. The best-fit curve to the experimental data, expressed in terms of strain amplitude ε_a (%) and fatigue cycles N, for CSs is given by

$$\ln[N] = 6.726 - 2.0 \ln(\varepsilon_a - 0.0722) \quad (9a)$$

and for LASs by

$$\ln[N] = 6.339 - 2.0 \ln(\varepsilon_a - 0.1283). \quad (9b)$$

The mean curve, expressed in terms of stress amplitude S_a (MPa), which is the product of ε_a and elastic modulus E, for CSs is given by

$$S_a = 59{,}736/\sqrt{N} + 149.24 \quad (10a)$$

and for LASs by

$$S_a = 49{,}222/\sqrt{N} + 265.45. \quad (10b)$$

The room–temperature value of 206.8 GPa (30,000 ksi) for the elastic modulus for carbon and low–alloy steels was used in converting the experimental strain–versus–life data to stress–versus–life curves. The best–fit curves were adjusted for the effect of mean stress by using the modified Goodman relation

$$S'_a = S_a\left(\frac{\sigma_u - \sigma_y}{\sigma_u - S_a}\right) \quad \text{for } S_a < \sigma_y, \tag{11a}$$

and

$$S'_a = S_a \qquad \text{for } S_a > \sigma_y, \tag{11b}$$

where S'_a is the adjusted value of stress amplitude, and σ_y and σ_u are yield and ultimate strengths of the material, respectively. The Goodman relation assumes the maximum possible mean stress and typically gives a conservative adjustment for mean stress, at least when environmental effects are not significant. The design fatigue curves were then obtained by lowering the adjusted best–fit curve by a factor of 2 on stress or 20 on cycles, whichever was more conservative, at each point on the curve. The same procedure has been used to develop design fatigue curves for LWR environments.

The design fatigue curves based on the statistical model for CSs and LASs in air at 288°C are shown in Fig. 7. For both steels, the current ASME Code curve is conservative relative to the curves obtained from the statistical model. For LASs, the difference between the two curves is insignificant, whereas for CSs, the fatigue lives predicted by the current Code curve at stress levels of 100–200 MPa (14.5–29 ksi) are lower by more than a factor of 3 than those predicted by the curve from the statistical model. Figure 8 shows the design curves for LWR environments under service conditions in which any one of the following critical threshold conditions is true: DO <0.05 ppm, strain rate ≥1%/s, temperature <150°C.

Figure 9 shows the design curves under service conditions where temperature and DO level are above the threshold value and the strain rate is <1%/s. The design fatigue curves

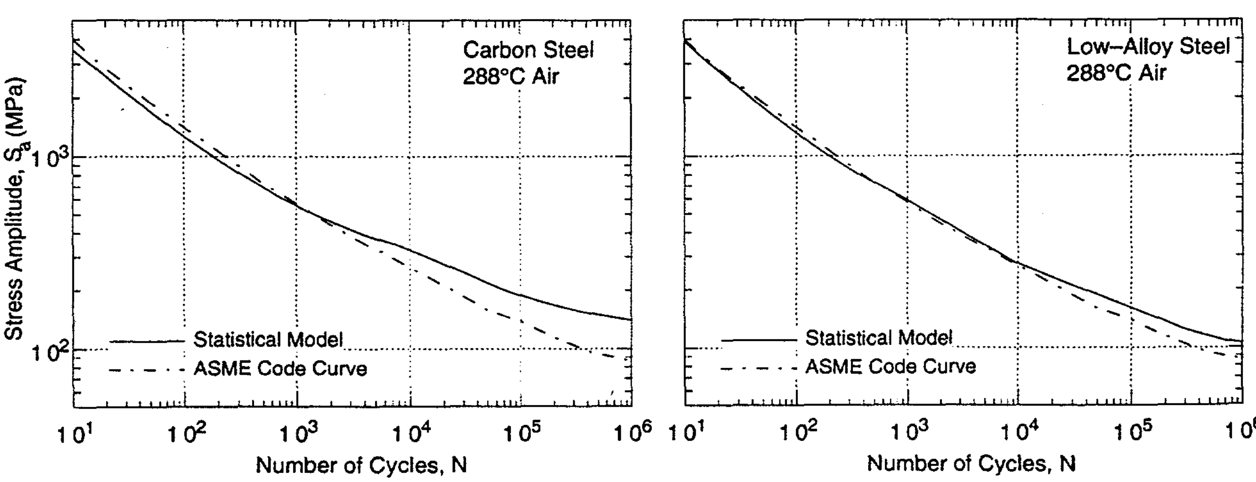

Figure 7. Fatigue design curves developed from statistical model for carbon and low–alloy steels in air at room temperature and 288°C

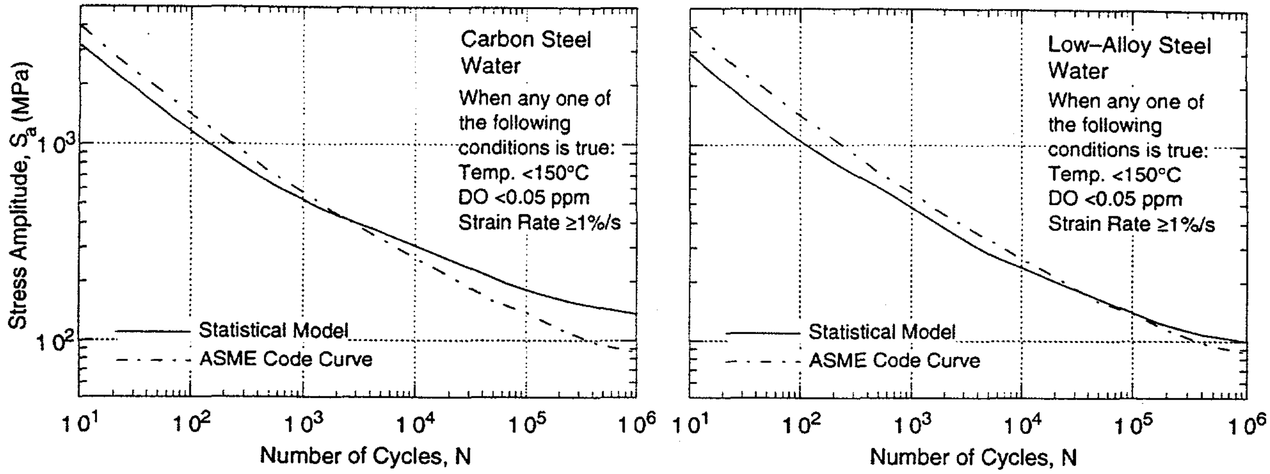

Figure 8. Fatigue design curves developed from statistical model for carbon and low–alloy steels under service conditions in which one or more threshold values are not satisfied

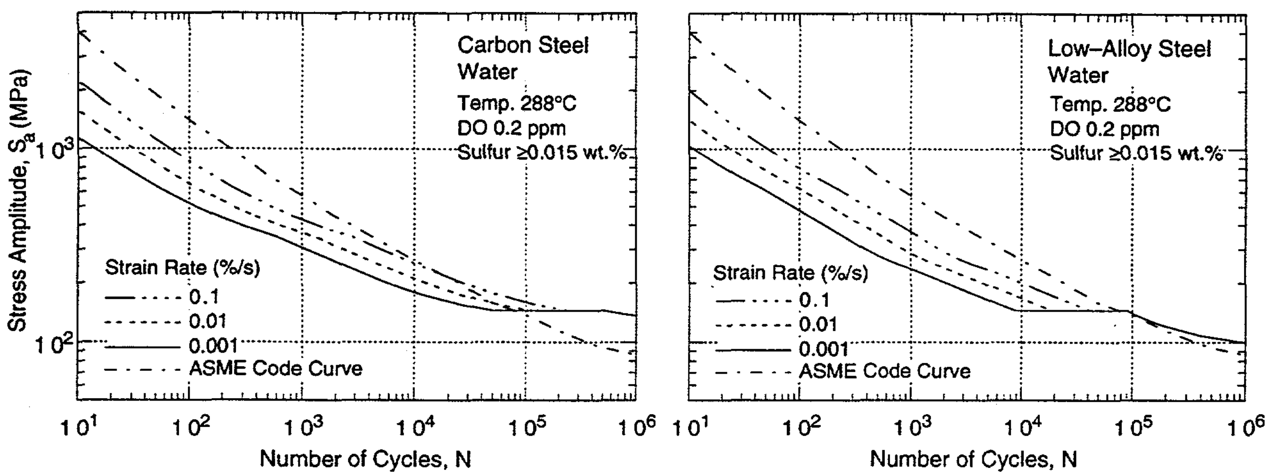

Figure 9. Fatigue design curves developed from statistical model for carbon and low–alloy steels under service conditions in which all critical threshold values are satisfied

corresponding to strain rates of 0.1, 0.01, and a saturation value of 0.001%/s, in water at 288°C are shown in the figure. A DO level of 0.2 ppm in water and high sulfur content (0.015 wt.% or higher) is assumed in the steels. Also, a minimum threshold strain amplitude of 0.07% (or a stress amplitude of 145 MPa) is defined, below which environmental effects are modest and are represented by the curves shown in Fig. 8. Note that these curves not only account for environmental effects but also include minor differences between the current ASME mean air curves and statistical model mean air curves that have been developed from a more extensive data base. Similar curves may be obtained for other service temperatures.

CONSERVATISM IN DESIGN FATIGUE CURVES

Structural Integrity Associates, Inc., under contract to Sandia National Laboratories for the U.S. Department of Energy, and in cooperation with the Electric Power Research Institute (EPRI),[41] have documented the types and extent of conservatisms present in the ASME Section III fatigue evaluations and the effects of LWR environments on fatigue margins. The sources of conservatism include design transients considerably more severe than those experienced in service, grouping of transients, simplified elastic–plastic analysis, and Code rules prior to 1979. Environmental effects on two components, the BWR feedwater nozzle/safe end and PWR steam generator feedwater nozzle/safe end, known to be affected by severe thermal transients, were also investigated in the study. It was concluded that the reductions in fatigue life due to environmental effects (factors of up to 40 and 22 for PWR and BWR nozzles, respectively) are more than offset by the margins in fatigue life (≈60 and 90, respectively, for PWR and BWR nozzles) found in typical ASME Code fatigue evaluations. The margins of ≈60 and 90 on fatigue life were determined from the ratio of CUFs based on the mean experimental S–N curve and the Code design fatigue curve. In other words, the factors of 2 on stress and 20 on cycles have been considered as safety margins in these evaluations. The margins of ≈60 and 90 would be true only if it was demonstrated that the fatigue S–N curve for these specific components was comparable to or better than the mean experimental curve, and that mean stress, loading sequence, or component size and geometry, have no effect on fatigue life.

The overall conservatism in ASME Code fatigue evaluations, however, has been demonstrated in fatigue tests on piping welds and components.[42] In air, the margins on the number of cycles to failure for elbows and tees were 118–2500 and 123–1700, respectively, for carbon steels. The margins for girth butt welds were significantly lower at 14–128. In these tests, fatigue life was expressed as the number of cycles for the crack to penetrate through the wall, which ranged from 6–18 mm (0.237–0.719 in.). The design fatigue curves represent the number of cycles to form a 3-mm-deep crack. Consequently, depending on wall thickness, the actual margins to failure may be lower by a factor of >2.

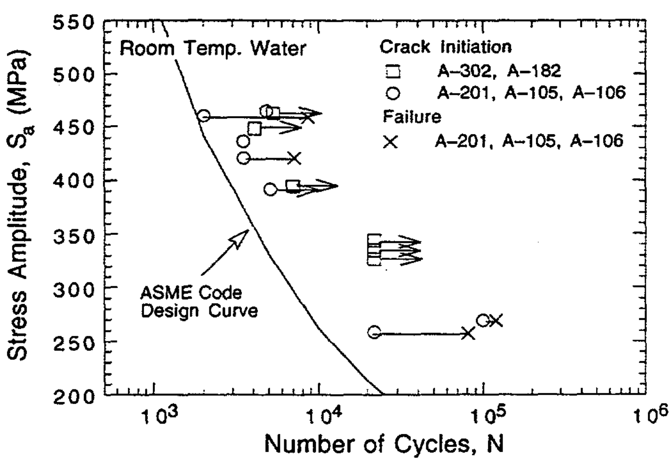

Figure 10.
Fatigue data for carbon and low-alloy steel vessels tested in room-temperature water

Most of the margin arises in the calculation of the stresses using the conventional Code procedures. These procedures are probably quite conservative for most fittings. Fatigue tests conducted on vessels at Southwest Research Institute for the PVRC[43] show that ≈5 mm deep cracks can form in carbon and low-alloy steels very close to the values predicted by the ASME Code design curve, Fig. 10. The tests were performed on 0.914 m (36 in.) diameter vessels with 19 mm (0.75 in.) wall in room-temperature water. These results demonstrate clearly that the Code design fatigue curves do not necessarily guarantee any margin of safety.

A PVRC working group has been compiling and evaluating fatigue S–N data related to the effects of LWR coolant environments on the fatigue life of pressure boundary materials.[4] One of the tasks in the PVRC activity consisted of defining a set of values for material, loading, and environmental variables that result in moderate or acceptable effects of environment on fatigue life. A factor of 4 on the ASME mean life was chosen as a working definition of "moderate" or "acceptable" effects of environment, i.e., up to a factor 4 decrease in fatigue life due to environment is considered acceptable and does not require further fatigue evaluation. The basis for this criterion is that a factor of 4 on life constitutes normal data scatter and/or there is at least that much conservatism in the design fatigue curves.

The results of a rigorous statistical analysis have been used to estimate the probability of forming fatigue cracks in CS and LAS components.[38,39] The results indicate that in room-temperature air, the current ASME Code design fatigue curve ensures that there is <5% probability of fatigue cracking in LAS components and <1% probability in CS components. Data available in the literature have been reviewed to evaluate the effects of various material, loading, and environmental variables on the fatigue life of structural materials in air and LWR environments.[38] The subfactors that may be used to account for the effects of these variables on fatigue life are summarized in Table 1. The factors on strain primarily account for the variation in fatigue limit of the material caused by material variability, component size and surface finish, and load history. The effects of these parameters on threshold strain are judged not to be cumulative but rather are controlled by the parameter that has the largest effect. Thus, a factor of at least 1.5 on strain and 10 on cycles is needed to account for the differences and uncertainties in relating the fatigue lives of laboratory test specimens to those of large components. In high-temperature water, the effect of surface finish may not be significant; both carbon and low-alloy steels develop a corrosion scale. For LWR environments, the subfactor on life to account for surface finish effects may be as low as 1.5 or may be eliminated completely. Therefore, a factor of 3 or 4 on life appears reasonable for defining moderate or acceptable effects of environment on fatigue life of carbon and low-alloy steels, consistent with the conclusions of the PVRC working group.

Table 1. Factors on cycles and on strain to be applied to mean S–N curve

Parameter	Factor on Life	Factor on Strain
Material variability & experimental scatter	2.5	1.4–1.7
Size effect	1.4	1.25
Surface finish	2.0–3.0	1.3
Loading history	1.5–2.5	1.5
Total adjustment:	10.0–26.0	1.5–1.7

FATIGUE EVALUATIONS IN LWR ENVIRONMENTS

The Section III, NB-3200- or NB-3600-type analyses for components for service in LWR environments can be performed using the design fatigue curves presented in Figs. 8 and 9. An alternative approach could be based on a fatigue life correction factor F_{en} proposed by EPRI[40] and the EFD committee of TENPES of Japan. In the EPRI approach, F_{en} is expressed as the ratio of the life in air to that in water, both at service temperature, whereas in the EFD approach, F_{en} is expressed as the ratio of the life in air at room temperature to that in water at service temperature. The effects of environment are incorporated into the ASME fatigue evaluation by obtaining a fatigue usage for a specific load pair based on the current Code design curves and multiplying it by the correction factor.

Both of these approaches require additional information regarding the service conditions, e.g., temperature, strain rate, and DO level. The procedure for obtaining these parameters depends on the details of the available information, i.e., whether the elapsed time versus temperature information for the transient is available. An average temperature may be used if the time vs. temperature information is available. Because environmental effects on fatigue life are modest at temperatures of <150°C and at strains below the threshold value, average temperature may be determined by the average of the maximum temperature and either 150°C or the temperature at threshold strain, whichever is higher. An average strain rate is generally used for each load state: it is obtained from the peak strain and elapsed time for the transient. However, fatigue monitoring data indicate that actual strain rates may vary significantly during the transient. The slowest strain rate can be used for a conservative estimate of life.

An "improved rate approach" has been proposed for obtaining the fatigue life correction factor F_{en} under conditions of varying temperature, strain rate, and DO level.[18] During each loading cycle, F_{en} is assumed to vary linearly with strain increments. The effective correction factor $F_{en}^{'}$ for varying conditions is expressed as

$$F_{en}^{'} = 1 + \int_{\varepsilon_{th}}^{\varepsilon_{max}} \frac{F_{en} - 1}{\varepsilon_{max} - \varepsilon_{th}} d\varepsilon, \tag{12}$$

where ε_{max} and ε_{th} are the maximum and threshold values of strain, respectively. For varying service conditions, Eq. 12 may be written in terms of the effective fatigue life in water $N_{water}^{'}$ expressed as

$$\frac{1}{N_{water}^{'}} = \int_{\varepsilon_{th}}^{\varepsilon_{max}} \frac{1}{N_{water}} \frac{d\varepsilon}{(\varepsilon_{max} - \varepsilon_{th})} \tag{13}$$

or

$$\frac{1}{N_{water}^{'}} = \int_{T_{th}}^{T_{max}} \frac{1}{N_{water}} \frac{dT}{(T_{max} - T_{th})}, \tag{14}$$

where N_{water} is the life under constant temperature and strain rate, and T_{max} and T_{th} are the maximum and threshold values of temperature, respectively.

Sample fatigue evaluations have been performed for a SA-508 Cl 1 CS feedwater nozzle safe end and SA-333 Gr 6 CS feedwater line piping for a BWR, and a SA-508 Cl 2 LAS outlet nozzle for a PWR vessel; the results are given in Tables 2-4. The stress records and the associated service conditions were obtained from Ref. 44. Three methods were used to calculate CUF for each set of load pair: (a) partial usage factor obtained from the appropriate design fatigue curve (examples are shown in Figs. 8 and 9); (b) obtain a partial usage factor from the current ASME Code design curve, then adjust the value for environmental effects by multiplying by F_{en}, which is calculated from Eqs. 8a and 8b; and (c) same procedure as in (b), except that F_{en} is calculated from Eqs. 4a-6d. F_{en} values were obtained for only those load pairs that satisfy the following three threshold conditions: temperature ≥150°C, strain rate ≤1%/s, and stress amplitude ≥145 MPa (≥21 ksi). A DO level of 0.2 ppm and sulfur content of 0.015 wt.% were assumed for these calculations. Also, σ_u in Eq. 6b was assumed to be 520 MPa for CSs and 650 MPa for LASs.

The results indicate that the approach using F_{en} yields higher values of CUF than those obtained from the design fatigue curves adjusted for environmental effects. The difference arises because the environmentally adjusted design curves account not only for the environment but also for the difference between the ASME mean air curve and statistical model

Table 4. *Fatigue evaluation for SA-508 Cl 2 low-alloy steel outlet nozzle for PWR*

S_{alt} (MPa)	Temp. (°C)	Strain Rate (%/s)	Design Cycles n	ASME Code Curve N	ASME Code Curve U_{air}	Curves Based on Statistical Model N	Curves Based on Statistical Model U_{env}	Correction Based on Statistical Model F_{en}	Correction Based on Statistical Model U_{env}	Correction Based on EFD Model F_{en}	Correction Based on EFD Model U_{env}
335.6	–	–	80	4670	0.0171	2573	0.0311	1.77	0.0303	–	–
313.0	–	–	10	5741	0.0017	3091	0.0032	1.77	0.0031	–	–
305.7	–	–	20	6010	0.0033	3388	0.0059	1.77	0.0059	–	–
275.4	–	–	20	8098	0.0025	4670	0.0043	1.77	0.0044	–	–
237.1	–	–	70	13723	0.0051	9508	0.0074	1.77	0.0090	–	–
202.1	–	–	130	23795	0.0055	24912	0.0052	1.77	0.0097	–	–
195.1	–	–	150	26082	0.0058	27939	0.0054	1.77	0.0102	–	–
186.8	–	–	50	29251	0.0017	32061	0.0016	1.77	0.0030	–	–
186.1	–	–	30	28587	0.0010	33566	0.0009	1.77	0.0019	–	–
147.3	–	–	40	68338	0.0006	76641	0.0005	1.77	0.0010	–	–
139.3	–	–	1930	94211	0.0205	94211	0.0205	1.00	0.0205	–	–
139.3	–	–	2000	94211	0.0212	94211	0.0212	1.00	0.0212	–	–
138.8	–	–	9270	94211	0.0984	94211	0.0984	1.00	0.0984	–	–
130.0	–	–	60	115810	0.0005	115810	0.0005	1.00	0.0005	–	–
127.1	–	–	230	132894	0.0017	129881	0.0018	1.00	0.0017	–	–
126.5	–	–	10	135977	0.0001	135977	0.0001	1.00	0.0001	–	–
124.5	–	–	80	142360	0.0006	149041	0.0005	1.00	0.0006	–	–
121.6	–	–	160	149041	0.0011	183210	0.0009	1.00	0.0011	–	–
121.6	–	–	26400	152499	0.1731	167150	0.1579	1.00	0.1731	–	–
117.6	–	–	2000	167150	0.0120	205470	0.0097	1.00	0.0120	–	–
113.0	–	–	400	191809	0.0021	252575	0.0016	1.00	0.0021	–	–
110.2	–	–	13200	215114	0.0614	310479	0.0425	1.00	0.0614	–	–
106.0	–	–	13200	241252	0.0547	364547	0.0362	1.00	0.0547	–	–
102.7	–	–	80	289835	0.0003	617784	0.0001	1.00	0.0003	–	–
102.3	–	–	80	289835	0.0003	603777	0.0001	1.00	0.0003	–	–
101.4	–	–	70	317682	0.0002	777031	0.0001	1.00	0.0002	–	–
					0.4924		0.4576		0.5266		

[a] Not calculated because strain rates were not available in the stress records.

air curve. F_{en} is based on the relative values of the statistical models in air and water, but applied to the ASME curve. Figure 7 show that for CSs, this difference can be significant at stress amplitudes <180 MPa (<26 ksi). The results also show that for the feedwater nozzle safe end and the feedwater line piping, the BWR environment increases the fatigue usage by a factor of ≈2. For the LAS outlet nozzle of a PWR, the effect environment on fatigue usage is insignificant. The CUF values from the EFD model were not calculated because information regarding the strain rate was not available in the stress records. For stress levels above ≈145 MPa (21 ksi), the EFD approach would yield F_{en} values of 1.25 and 1.95 for strain rates of 0.1 and 0.001%/s, respectively.

SUMMARY

The work performed at ANL on fatigue of carbon and low-alloy steels in LWR environments is summarized. The existing fatigue S-N data have been evaluated to establish the effects of various material and loading variables such as steel type, strain range, strain rate, temperature, sulfur content in steel, orientation, and DO level in water on the fatigue life of these steels. The influence of reactor environments on fatigue crack initiation is discussed. The decrease in fatigue life of carbon and low-alloy steels in high-DO water is primarily caused by the effects of environment on the growth of short cracks < 100 μm deep. In LWR

environments, the results indicate that the growth of short fatigue cracks occurs by a slip oxidation/dissolution process. Statistical models have been developed for estimating the fatigue S–N curves as a function of material, loading, and environmental variables. Design fatigue curves have been developed for carbon and low–alloy steel components in LWR environments. Alternative methods for incorporating the effects of LWR coolant environments into the ASME Code fatigue evaluations are presented. Sample fatigue evaluations have been performed for selected reactor components by using either the design fatigue curves based on the statistical model or by applying a fatigue life correction factor.

ACKNOWLEDGMENTS

This work was sponsored by the Office of Nuclear Regulatory Research, U.S. Nuclear Regulatory Commission, FIN Number W6610; Program Manager: Dr. M. McNeil.

REFERENCES

1. Ranganath, S., Kass, J. N., and Heald, J. D., "Fatigue Behavior of Carbon Steel Components in High–Temperature Water Environments," in *BWR Environmental Cracking Margins for Carbon Steel Piping*, EPRI NP–2406, Electric Power Research Institute, Palo Alto, CA, Appendix 3, May 1982.

2. Higuchi, M., and Iida, K., "Fatigue Strength Correction Factors for Carbon and Low–Alloy Steels in Oxygen–Containing High–Temperature Water," *Nucl. Eng. Des.* **129**, pp. 293–306, 1991.

3. Van Der Sluys, W. A., "Evaluation of the Available Data on the Effect of the Environment on the Low Cycle Fatigue Properties in Light Water Reactor Environments," in *Proc. 6th Intl. Symp. on Environmental Degradation of Materials in Nuclear Power Systems – Water Reactors*, R. E. Gold and E. P. Simonen, eds., The Metallurgical Society, Warrendale, PA, pp. 1–4, 1993.

4. Van Der Sluys, W. A., and Yukawa, S., "Status of PVRC Evaluation of LWR Coolant Environmental Effects on the S–N Fatigue Properties of Pressure Boundary Materials," in *Fatigue and Crack Growth: Environmental Effects, Modeling Studies, and Design Considerations*, S. Yukawa, ed., American Society of Mechanical Engineers, New York, pp. 47–58, 1995.

5. Chopra, O. K., and Shack, W. J., "Evaluation of Effects of LWR Coolant Environments on Fatigue Life of Carbon and Low–Alloy Steels," in *Effects of the Environment on the Initiation of Crack Growth*, ASTM STP 1298, W. A. Van Der Sluys, R. S. Piascik, and R. Zawierucha, eds., American Society for Testing and Materials, Philadelphia, pp. 247–266, 1997.

6. Hale, D. A., Wilson, S. A., Kiss, E., and Gianuzzi, A. J., "Low Cycle Fatigue Evaluation of Primary Piping Materials in a BWR Environment," GEAP–20244, U.S. Nuclear Regulatory Commission, Sept. 1977.

7. Hale, D. A., Wilson, S. A., Kass, J. N., and Kiss, E., "Low Cycle Fatigue Behavior of Commercial Piping Materials in a BWR Environment," *J. Eng. Mater. Technol.* **103**, 15–25, 1981.

8. Terrel, J. B., "Fatigue Strength of Smooth and Notched Specimens of ASME SA 106-B Steel in PWR Environments," NUREG/CR-5136, MEA-2289, Materials Engineering Associates, Inc., Lanham, MD, Sept. 1988.

9. Terrel, J. B., "Effect of Cyclic Frequency on the Fatigue Life of ASME SA 106-B Piping Steel in PWR Environments," *J. Mater. Eng.* **10**, 193-203, 1988.

10. Chopra, O. K., and Shack, W. J., "Effects of LWR Environments on Fatigue Life of Carbon and Low-Alloy Steels," in *Fatigue and Crack Growth: Environmental Effects, Modeling Studies, and Design Considerations*, PVP Vol. 306, S. Yukawa, ed., American Society of Mechanical Engineers, New York, pp. 95-109, 1995.

11. Chopra, O. K., and Shack, W. J., "Effects of Material and Loading Variables on Fatigue Life of Carbon and Low-Alloy Steels in LWR Environments," in *Transactions of 13th Int. Conf. on Structural Mechanics in Reactor Technology (SMiRT 13)*, Vol. II, M. M. Rocha and J. D. Riera, eds., Escola de Engenharia - Universidade Federal do Rio Grande do Sul, Porto Alegre, Brazil, pp. 551-562, 1995.

12. Chopra, O. K., and Shack, W. J., "Effects of LWR Coolant Environments on Fatigue S-N Curves for Carbon and Low-Alloy Steels," in *Pressure Vessel and Piping Code and Standards*, PVP Vol. 339, T. S. Esselman, ed., American Society of Mechanical Engineers, New York, pp. 185-198, 1996.

13. Gavenda, D. J., Luebbers, P. R., and Chopra, O. K., "Crack Initiation and Crack Growth Behavior of Carbon and Low-Alloy Steels," in *Fatigue and Fracture 1*, Vol. 350, S. Rahman, K. K. Yoon, S. Bhandari, R. Warke, and J. M. Bloom, eds., American Society of Mechanical Engineers, New York, pp. 243-255,1997.

14. Nagata, N., Sato, S., and Katada, Y., "Low-Cycle Fatigue Behavior of Pressure Vessel Steels in High-Temperature Pressurized Water," *ISIJ Intl.* **31** (1), 106-114, 1991.

15. Katada, Y., Nagata, N., and Sato, S., "Effect of Dissolved Oxygen Concentration on Fatigue Crack Growth Behavior of A533 B Steel in High-Temperature Water," *ISIJ Intl.* **33** (8), 877-883, 1993.

16. Higuchi, M., Iida, K., and Asada, Y., "Effects of Strain Rate Change on Fatigue Life of Carbon Steel in High-Temperature Water," in *Fatigue and Crack Growth: Environmental Effects, Modeling Studies, and Design Considerations*, PVP Vol. 306, S. Yukawa, ed., American Society of Mechanical Engineers, New York, pp. 111-116, 1995; also in *Effects of the Environment on the Initiation of Crack Growth*, ASTM STP 1298, W. A. Van Der Sluys, R. S. Piascik, and R. Zawierucha, eds., American Society for Testing and Materials, Philadelphia, pp. 216-231, 1997.

17. Nakao, G., Kanasaki, H., Higuchi, M., Iida, K., and Asada, Y., "Effects of Temperature and Dissolved Oxygen Content on Fatigue Life of Carbon and Low-Alloy Steels in LWR Water Environment," in *Fatigue and Crack Growth: Environmental Effects, Modeling Studies, and Design Considerations*, PVP Vol. 306, S. Yukawa, ed., American Society of Mechanical Engineers, New York, pp. 123-128, 1995.

18. Kanasaki, H., Hayashi, M., Iida, K., and Asada, Y., "Effects of Temperature Change on Fatigue Life of Carbon Steel in High-Temperature Water," in *Fatigue and Crack Growth: Environmental Effects, Modeling Studies, and Design Considerations*, PVP Vol. 306, S. Yukawa, ed., American Society of Mechanical Engineers, New York, pp. 117–122, 1995.

19. Ford, F. P., Ranganath, S., and Weinstein, D., "Environmentally Assisted Fatigue Crack Initiation in Low-Alloy Steels – A Review of the Literature and the ASME Code Design Requirements," EPRI Report TR-102765, Aug. 1993.

20. Pleune, T. T., and Chopra, O. K., "Artificial Neural Networks and Effects of Loading Conditions on Fatigue Life of Carbon and Low-Alloy Steels," in *Fatigue and Fracture 1*, Vol. 350, S. Rahman, K. K. Yoon, S. Bhandari, R. Warke, and J. M. Bloom, eds., American Society of Mechanical Engineers, New York, pp. 413–423, 1997.

21. Cullen, W. H., Kemppainen, M., Hänninen, H., and Törrönen, K., "The Effects of Sulfur Chemistry and Flow Rate on Fatigue Crack Growth Rates in LWR Environments," NUREG/CR-4121, 1985.

22. Bulloch, J. H., "A Review of Fatigue Crack Extension Behavior of Ferritic Reactor Pressure Vessels Materials in Pressurized Water Reactor Environments," Res. Mech. **26**, pp. 95–172, 1989.

23. Van Der Sluys, W. A., and Emanuelson, R. H., "Environmental Acceleration of Fatigue Crack Growth in Reactor Pressure Vessel Materials," EPRI Report TR-102796, Aug. 1993.

24. Atkinson, J. D., Yu, J., and Chen, Z.-Y., "An Analysis of the Effects of Sulfur Content and Potential on Corrosion Fatigue Crack Growth in Reactor Pressure Vessel Steels," *Corros. Sci.* **38** (5), pp. 755–765, 1996.

25. Wire, G. L., and Li, Y. Y., "Initiation of Environmentally-Assisted Cracking in Low-Alloy Steels," in *Fatigue and Fracture Volume 1*, PVP Vol. 323, H. S. Mehta, ed., American Society of Mechanical Engineers, New York, pp. 269–289, 1996.

26. Chopra, O. K., Gavenda, D. J., and Shack, W. J., "Fatigue of Ferritic Steels," in *Environmentally Assisted Cracking in Light Water Reactors, Semiannual Report, October 1994–March 1995*, NUREG/CR-4667, Vol. 20, ANL-95/41, pp. 1–19, Jan. 1996.

27. James, L. A., "The Effect of Water Flow Rate Upon the Environmentally-Assisted Cracking Response of a Low-Alloy Steel," *J. Pressure Vessel Technol.* **117** (3), pp. 238–244, 1995.

28. Chopra, O. K., Michaud, W. F., Shack, W. J., and Soppet, W. K., "Fatigue of Ferritic Steels," in *Environmentally Assisted Cracking in Light Water Reactors, Semiannual Report, April–September 1993*, NUREG/CR-4667, Vol. 17, ANL-94/16, pp. 1–22, June 1994.

29. Miller, K. J., "Damage in Fatigue: A New Outlook," in *International; Pressure Vessels and Piping Codes and Standard: Volume 1 – Current Applications*, PVP Vol. 313-1, K. R. Rao and Y. Asada, eds., American Society of Mechanical Engineers, New York, pp. 191–192, 1995.

30. C. M. Suh, R. Yuuki, and H. Kitagawa, "Fatigue Microcracks in a Low Carbon Steel," *Fatigue Fract. Engng. Mater. Struct.* **8**, 193–203 (1985).

31. Tokaji, K., Ogawa, T., and Osako, S., "The Growth of Microstructurally Small Fatigue Cracks in a Ferritic–Pearlitic Steel," *Fatigue Fract. Engng. Mater. Struct.* **11**, pp. 331–342, 1988.

32. Tokaji, K., and Ogawa, T., "The Growth of Microstructurally Small Fatigue Cracks in Metals," in *Short Fatigue Cracks*, ESIS 13, M. J. Miller and E. R. de los Rios, eds., Mechanical Engineering Publication, London, pp. 85–99, 1992.

33. de los Rios, E. R., Tang, Z., and Miller, K. J., "Short Crack Fatigue Behavior in a Medium Carbon Steel," *Fatigue Fract. Engng. Mater. Struct.* **7**, pp, 97–108, 1984.

34. de los Rios, E. R., Navarro, A., and Hussain, K., "Microstructural Variations in Short Fatigue Crack Propagation of a C–Mn Steel," in *Short Fatigue Cracks*, ESIS 13, M. J. Miller and E. R. de los Rios, eds., Mechanical Engineering Publication, London, pp. 115–132, 1992.

35. Atkinson, J. D., Bulloch, J. H., and Forrest, J. E., "A Fractographic Study of Fatigue Cracks Produced in A533B Pressure Vessel Steel Exposed to Simulated PWR Primary Water Environments," in *Proc. 2nd Int. Atomic Energy Agency Specialists' Meeting on Subcritical Crack Growth*, NUREG/CP–0067, MEA–2090, Vol. 2, pp. 269–290, April 1986.

36. K. Törrönen, M. Kempainen, and H. Hänninen, *Fractographic Evaluation of Specimens of A533B Pressure Vessel Steel*, EPRI Report NP–3483, Project 1325–7, (May 1984).

37. Eason, E. D., Nelson, E. E., and Gilman, J. D., "Modeling of Fatigue Crack Growth Rate for Ferritic Steels in Light Water Reactor Environments," in *Changing Priorities of Code and Standards*, PVP–Vol. 286, ASME, pp. 131–142, 1994.

38. Keisler, J., Chopra, O. K., and Shack, W. J., "Fatigue Strain–Life Behavior of Carbon and Low–Alloy Steels, Austenitic Stainless Steels, and Alloy 600 in LWR Environments," NUREG/CR–6335, ANL–95/15, Aug. 1995.

39. Keisler, J., Chopra, O. K., and Shack, W. J., "Fatigue Strain–Life Behavior of Carbon and Low–Alloy Steels, Austenitic Stainless Steels, and Alloy 600 in LWR Environments," *Nucl. Eng. Des.* **167**, pp. 129–154, 1996.

40. Mehta, H. S., and Gosselin, S. R., "An Environmental Factor Approach to Account for Reactor Water Effects in Light Water Reactor Pressure Vessel and Piping Fatigue Evaluations," in *Fatigue and Fracture Volume 1*, PVP Vol. 323, H. S. Mehta, ed., American Society of Mechanical Engineers, New York, pp. 171–185, 1996.

41. Deardorff, A. F., and Smith, J. K., "Evaluation of Conservatisms and Environmental Effects in ASME Code, Section III, Class 1 Fatigue Analysis," SAND94–0187, prepared by Structural Integrity Associates, San Jose, CA, underr contract to Sandia National Laboratories, Albuquerque, NM, Aug. 1994.

42. Mayfield, M. E., Rodabaugh, E. C., and Eiber, R. J., "A Comparison of Fatigue Test Data on Piping with the ASME Code Fatigue Evaluation Procedure," ASME paper 79-PVP-92, American Society of Mechanical Engineers, New York, 1979.

43. Kooistra, L. F., Lange, E. A., and Pickett, A. G., "Full-Size Pressure Vessel Testing and Its Application to Design," *J. Eng. Power* **86**, pp. 419–428, 1964.

44. Ware, A. G., Morton, D. K., and Nitzel, M. E., "Application of NUREG/CR-5999 Interim Design Curves to Selected Nuclear Power Plant Components," NUREG/CR-6260, INEL-95/0045, March 1995.